CSIRO PUBLISHING

Australian Journal of Physics

Volume 53, 2000

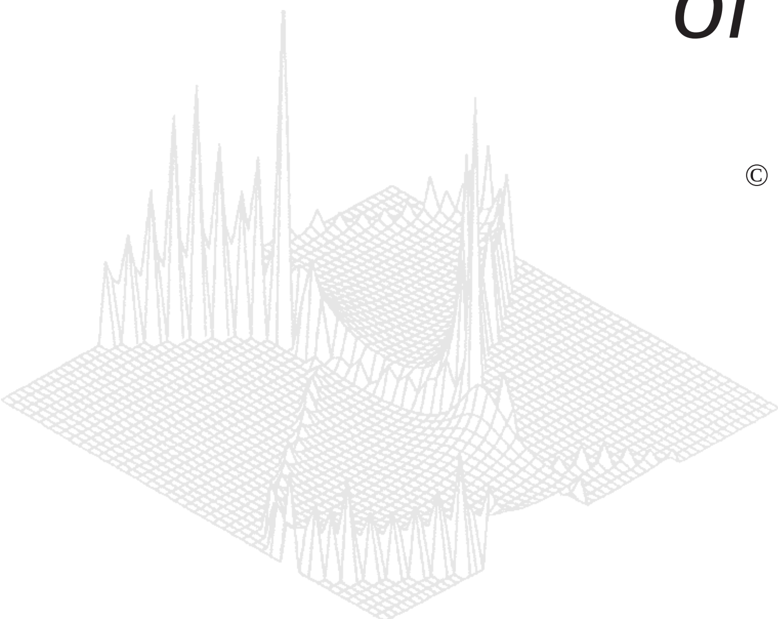

A journal for the publication of
original research in all branches of physics

www.publish.csiro.au/journals/ajp

All enquiries and manuscripts should be directed to
Australian Journal of Physics
CSIRO PUBLISHING
PO Box 1139 (150 Oxford St)
Collingwood
Vic. 3066
Australia

Telephone: 61 3 9662 7626
Facsimile: 61 3 9662 7611
Email: peter.robertson@publish.csiro.au

Published by **CSIRO** PUBLISHING
for CSIRO Australia and
the Australian Academy of Science

Aust. J. Phys., 2000, **53**, 333–44

On the Radiative Instability

E. T. Rowe and G. W. Rowe[A]

Special Research Centre for Theoretical Astrophysics,
School of Physics, University of Sydney, NSW 2006, Australia.
[A] Present address: 43 Yarram St ,
Lidcombe, NSW 2141, Australia.

Abstract

A thin beam of monoenergetic electrons and positrons may be described by a single interface with a surface current and it is shown that wave modes (in particular their growth rates) depend only on the form of this surface current and not explicitly on the geometry, specifically whether it is planar or cylindrical. We give general results for the wave modes which reproduce those previously obtained in the planar and cylindrical geometries and discuss their implications.

1. Introduction

The possibility of coherent synchrotron emission from a uniform distribution of charges moving around a thin circular ring of width a surrounded by vacuum was considered by Goldreich and Keeley (1971). Their method involved calculating the effect of the radiation fields of a distribution of charged particles on other given particles. Growing perturbations were therefore referred to as radiative instabilities. The coherence was shown by Buschauer and Benford (1978) to be due to a form of reactive growth involving negative particle energy in the ring.

More recently, Asséo *et al.* (1983) and Asséo (1995) (hereinafter referred to as APS83 and A95 respectively) appear to have reproduced this radiative instability. In their analysis the ring of moving charged particles is modelled as a strongly magnetised cold pair plasma annulus (or beam) bounded on two sides by other plasmas. A dispersion equation for wave perturbations is derived by enforcing electromagnetic boundary conditions at the plasma interfaces, and the Goldreich–Keeley form of the radiative instability is obtained if the bounding plasmas are replaced by vacuum. APS83 showed that particle motion along curved magnetic field lines alone is not enough to give instability and argued that the sharp boundaries they introduce are essential. It has also been suggested, however, that instability is due to the acceleration of plasma around the ring (Buschauer and Benford 1978).

In all of the calculations referred to above cylindrical geometry was assumed. Rowe and Rowe (1999*a*, 1999*b*) (hereinafter RR99) considered in detail thin beam modes for a strongly magnetised cold pair plasma slab (beam) surrounded by exterior plasmas in planar geometry, following the approach of APS83. As expected, radiative instability arises if there is a relative flow between the beam

 10.1071/PH99069 0004-9506/00/030333$05.00

and the bounding plasmas; however, if the exterior plasmas are replaced by vacuum there are only radiative modes which *damp* out perturbations.

In this paper we show that a thin beam surrounded by bounding plasmas may be regarded as a single infinitesimally thin current carrying interface between the bounding plasmas and we obtain an analytic expression for the frequency and growth rate of wave perturbations which is applicable to both planar and cylindrical geometry. The results indicate that it is the electromagnetic fields at this interface that determine the stability or instability of the beam, while its geometry is unimportant. In reality it is quite difficult to determine what the electromagnetic fields at the interface may be in an application to phenomena such as radio emission from pulsar magnetospheres. One approach is to choose the fields at the interface with a particular global geometry in mind, for example planar geometry (RR99) or cylindrical geometry (APS83). We show that our more general result reproduces these specific cases, in a straightforward manner.

The paper is set out as follows. In Section 2 we give a general dispersion equation for waves propagating along a strongly magnetised cold pair plasma beam surrounded by external plasmas. The dispersion equation is written in terms of the fields at the two plasma boundaries, in a form which is valid for planar and cylindrical geometries and for thick and thin beams. In Section 3 we consider thin beam wave modes and obtain the frequency and growth rate to $O(a^{\frac{1}{2}})$ (where a is the beam thickness) in a straightforward manner, showing that they depend only on the values of the electromagnetic fields at the beam and are independent of its geometry. In Section 4 we show that the general thin beam result reproduces previously reported planar geometry results as well as the radiative instability obtained in the cylindrical geometry. In Section 5 we interpret the results in terms of wave and particle energetics.

2. General Dispersion Equation

The general dispersion equation is obtained in terms of planar geometry but is equally valid for cylindrical geometry as discussed below. As in RR99, we consider a neutral beam of cold electrons and positrons flowing with speed U along a strong magnetic field relative to bounding electron–positron plasmas with different number densities. We use a coordinate system (x, y, z) with basis vectors $(\hat{\boldsymbol{x}}, \hat{\boldsymbol{y}}, \hat{\boldsymbol{z}})$, where $\hat{\boldsymbol{x}}$ is normal to the beam interface and $\hat{\boldsymbol{y}}$ is parallel to the magnetic field (note though that in RR99 $\hat{\boldsymbol{z}}$ is parallel to the magnetic field). The beam boundaries are located at $x = x_-$ and $x = x_+$.

The dielectric tensors in each of the media have the form $\boldsymbol{K}(\omega, \boldsymbol{k}) = (W-1)\hat{\boldsymbol{y}}\hat{\boldsymbol{y}}+\boldsymbol{\delta}$, with $\boldsymbol{\delta}$ the unit tensor and where for the beam plasma

$$W = W_b = 1 - \frac{\omega_p^2}{\gamma_p^3(\omega - k_y U)^2}\,, \tag{1}$$

while for the plasmas on the left and right of the beam (see Fig. 1)

$$W = W_l = 1 - \frac{\omega_{pl}^2}{\omega^2} \qquad \text{and} \qquad W = W_r = 1 - \frac{\omega_{pr}^2}{\omega^2}\,, \tag{2}$$

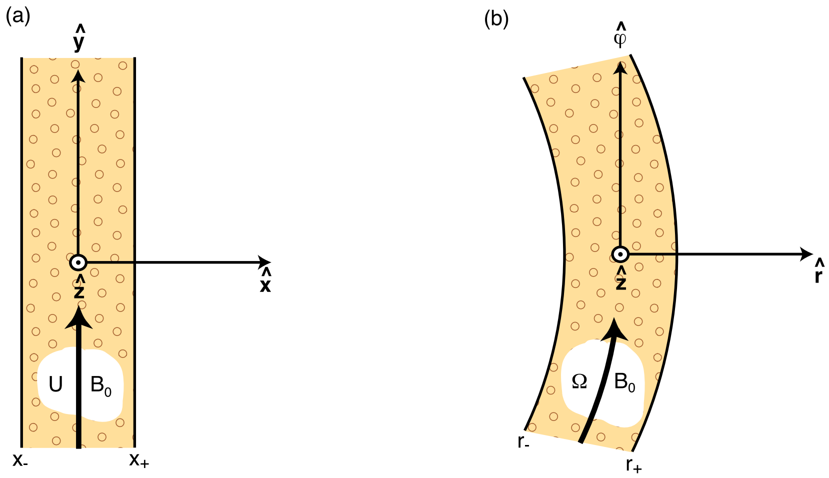

Fig. 1. The (a) planar and (b) cylindrical coordinate systems describing a beam. In the planar coordinate system the background magnetic field and beam flow are in the $\hat{\boldsymbol{y}}$ direction, while in the cylindrical coordinate system they are taken to be in the $\hat{\boldsymbol{\phi}}$ direction, as in APS83 and A95. In the text we refer to the bounding plasmas as the media on the left-hand and right-hand sides of the beam (subscripts l and r respectively), as suggested by the figure.

respectively. The Lorentz factor of the beam plasma is γ_p and ω_p, ω_{pl} and ω_{pr} are the total plasma frequencies in the beam and on the left and right of the beam respectively.

There are two wave modes in each plasma, one of which is a vacuum mode that can be neglected in the case $k_z = 0$ treated herein. The magnetic fields in each plasma have the form

$$\boldsymbol{B}(t, \boldsymbol{x}) = B(\omega, \rho) \exp\{i(k_y y - \omega t)\} \hat{\boldsymbol{z}}\,, \tag{3}$$

with the opposite sign convention in the temporal Fourier transform to that of APS83, and we use a dimensionless position variable $\rho = x/x_0$ where x_0 is a suitable scale length. The magnetic field inside the beam may in general be written as a linear combination of two linearly independent solutions $S^b_\alpha(\omega, \rho)$ and $S^b_\beta(\omega, \rho)$ in the remaining wave mode,

$$B^b(\omega, \rho) = \alpha S^b_\alpha(\omega, \rho) + \beta S^b_\beta(\omega, \rho)\,, \tag{4}$$

where α and β are arbitrary constants (independent of ρ). In each medium the wave electric field is determined by the equations

$$E_x = -\frac{k_y c^2}{\omega} B_z, \qquad E_y = -\frac{ic^2}{\omega W}\frac{\partial B_z}{\partial x} \qquad \text{and} \qquad E_z = 0\,. \tag{5}$$

The corresponding results for the cylindrical coordinate system are obtained by making the replacements $\hat{\boldsymbol{x}} \to \hat{\boldsymbol{r}}$ and $\hat{\boldsymbol{y}} \to \hat{\boldsymbol{\phi}}$ as suggested by Fig. 1, and $k_y \to m/r$, $y \to r\phi$, $\partial/\partial x \to \partial/\partial r$ and $U \to r\Omega$, where Ω is the angular velocity of the beam flow and m is the azimuthal wavenumber. Specific solutions for $B(\omega, \rho)$ in each medium have been given by RR99 for the planar geometry and APS83 for cylindrical geometry (see also Section 4).

The general dispersion equation is obtained by applying boundary conditions on the waves at both of the beam–plasma boundaries and eliminating α and β. As discussed in RR99 and APS83 the relevant boundary conditions are continuity of the tangential (to the interfaces) components of the electric and magnetic fields.

We define a function $\Pi_b(\omega, \rho_+, \rho_-)$ by

$$\Pi_b(\omega, \rho_+, \rho_-) = \frac{S^b_\alpha(\omega, \rho_+)S^b_\beta(\omega, \rho_-) - S^b_\alpha(\omega, \rho_-)S^b_\beta(\omega, \rho_+)}{W_b^2}\,, \tag{6}$$

with $\rho_+ = x_+/x_0$ (or r_+/r_0) and $\rho_- = x_-/x_0$ (or r_-/r_0), incorporating the solutions inside the beam. The reason for this definition will become clear in the next section. The dispersion equation can be written in the general form

$$\begin{aligned}
&\frac{W_b^2 B^{r(0,1)}(\omega, \rho_+)B^{l(0,1)}(\omega, \rho_-)}{W_r W_l}\Pi_b(\omega, \rho_+, \rho_-) \\
&-\frac{W_b B^{r(0,1)}(\omega, \rho_+)B^{l}(\omega, \rho_-)}{W_r}\Pi_b^{(0,0,1)}(\omega, \rho_+, \rho_-) \\
&-\frac{W_b B^{l(0,1)}(\omega, \rho_-)B^{r}(\omega, \rho_+)}{W_l}\Pi_b^{(0,1,0)}(\omega, \rho_+, \rho_-) \\
&+B^l(\omega, \rho_-)B^r(\omega, \rho_+)\Pi_b^{(0,1,1)}(\omega, \rho_+, \rho_-) = 0,
\end{aligned} \tag{7}$$

where B^l and B^r are the magnetic fields on the left and right sides of the beam. Partial derivatives are indicated by a superscripted parentheses notation, with the first element in parentheses giving the number of partial derivatives with respect to the first variable in the function and so on. We emphasise that the above approach is valid for both planar and cylindrical geometry and that the dispersion equation in this form reproduces those obtained in both geometries.

3. Thin Beam Solutions: Small a Approximation

Given specific functional forms for the magnetic fields, the general dispersion equation (7) may be solved numerically for the wave frequency ω. Analytic results may be obtained in the thin beam case by means of an expansion in $\delta = a/x_0 \ll 1$ where $a = x_+ - x_-$ is the beam thickness (again results obtained in terms of planar geometry apply also to cylindrical geometry with the substitutions of Section 2). It is known from APS83 and RR99 that in both the planar and cylindrical geometries thin beam solutions exist for the frequency of the form $\omega = \omega_R + \delta\omega + O[(\delta\omega)^2]$, where $\omega_R = k_y U$ is the beam resonance frequency and $\delta\omega \sim O(a^{\frac{1}{2}})$. We show here how the general approach incorporates and extends these geometry specific cases. The reality condition implies we need only consider $\omega_R > 0$ and without loss of generality we take $U > 0$ and $k_y > 0$ in the remainder of this paper.

The dielectric constant W_b varies for small $\delta\omega$ according to

$$W_b \approx -\frac{\omega_p^2}{\gamma_p^3(\delta\omega)^2}\left[1 + O(\delta\omega)\right] , \tag{8}$$

and in both the planar and cylindrical geometries the functions $S_\alpha^b(\omega,\rho)$ and $S_\beta^b(\omega,\rho)$ depend on W_b in such a way that an expansion of these functions in $\delta\omega$ (or in δ) is not possible, there being an essential singularity for $\delta\omega \to 0$ (or $\delta \to 0$). The function $\Pi_b(\omega,\rho_+,\rho_-)$ however has been defined so that it, and its derivatives appearing in (7), have Taylor expansions about $\delta = 0$. It is thus possible to solve the dispersion equation to any order in δ.

An alternative approach, valid to $O(a^{\frac{1}{2}})$, avoids direct calculation of the function $\Pi_b(\omega,\rho_+,\rho_-)$ and its expansions by treating the induced beam current as an infinitesimally thin surface current between the two bounding plasmas. In the Cartesian coordinate system the beam current is then equivalent to a surface current

$$\boldsymbol{J}_s(\omega) = i\varepsilon_0\omega a(1 - W_b)E_{sy}(\omega)\hat{\boldsymbol{y}} , \tag{9}$$

with $E_{sy}(\omega)$ given by the average of the y component of the electric field across the beam. This surface current leads to a discontinuity in the magnetic fields across the beam given by

$$J_s(\omega) = \frac{1}{\mu_0}\{B^l(\omega,\rho_-) - B^r(\omega,\rho_+)\} , \tag{10}$$

but the surface components of the electric field remain continuous.

Applying these boundary conditions to the wave fields in the two media, writing

$$B^r(\omega,\rho) = A(\omega)S^r(\omega,\rho) \qquad \text{and} \qquad B^l(\omega,\rho) = C(\omega)S^l(\omega,\rho) \tag{11}$$

and solving for the coefficients $A(\omega)$ and $C(\omega)$, one can write the resulting dispersion equation in the form

$$\begin{aligned} &\frac{\delta(1-W_b)}{W_l W_r}\,\frac{\partial B^r(\omega,\rho)}{\partial\rho}\,\frac{\partial B^l(\omega,\rho)}{\partial\rho} \\ &\quad - \frac{B^l(\omega,\rho)}{W_r}\,\frac{\partial B^r(\omega,\rho)}{\partial\rho} + \frac{B^r(\omega,\rho)}{W_l}\,\frac{\partial B^l(\omega,\rho)}{\partial\rho} = 0 . \end{aligned} \tag{12}$$

This dispersion equation is much simpler than (7), as the beam quantities appear only via W_b, whereas in (7) the magnetic field within the beam also appears explicitly via $\Pi_b(\omega,\rho_+,\rho_-)$. Equation (12) is not, however, as general as (7) and is not applicable to thick beams.

Writing $\delta\omega \approx \omega_{\frac{1}{2}}\delta^{\frac{1}{2}}$ and expanding (12) to $O(\delta^{\frac{1}{2}})$ one obtains

$$\omega_{\frac{1}{2}}^2 = \frac{\omega_p^2 B^{r(0,1)}(\omega_R,\rho_-)B^{l(0,1)}(\omega_R,\rho_-)}{\gamma_p^3[W_l B^l(\omega_R,\rho_-)B^{r(0,1)}(\omega_R,\rho_-) - W_r B^r(\omega_R,\rho_-)B^{l(0,1)}(\omega_R,\rho_-)]} , \tag{13}$$

where W_l and W_r are evaluated at $\omega = \omega_R$. This simplifies further in the case of identical external media ($\omega_{pr} = \omega_{pl}$) to

$$\omega_{\frac{1}{2}}^2 = \frac{\omega_R^2 \omega_p^2 B^{r(0,1)}(\omega_R, \rho_-) B^{l(0,1)}(\omega_R, \rho_-)}{\gamma_p^3(\omega_R^2 - \omega_{pl}^2)\mathcal{W}[B^l(\omega_R, \rho_-), B^r(\omega_R, \rho_-)]}\,, \tag{14}$$

with $\mathcal{W}[B^l, B^r]$ denoting the Wronskian of B^l and B^r (differentiation with respect to ρ_-). These results depend only on the magnetic fields in the bounding plasmas close to the beam and evaluated at the resonance frequency. They do not depend on the magnetic field in the beam or explicitly on the beam geometry. We only consider the case of identical bounding media in the remainder of this paper.

4. Specific Results

If the bounding media are identical ($W_l = W_r = W$), the most general form of the magnetic fields in planar geometry is

$$B^r(\omega, \rho) = a(\omega)\exp\{ik_x(\rho - 1)x_0\} + b(\omega)\exp\{-ik_x(\rho - 1)x_0\}\,, \tag{15}$$

$$B^l(\omega, \rho) = c(\omega)\exp\{ik_x(\rho - 1)x_0\} + d(\omega)\exp\{-ik_x(\rho - 1)x_0\}\,, \tag{16}$$

with $a(\omega)$, $b(\omega)$, $c(\omega)$, and $d(\omega)$ arbitrary functions of ω and

$$k_x^2 = \frac{\omega^2}{c^2} W\left(1 - \frac{c^2 k_y^2}{\omega^2}\right). \tag{17}$$

One finds

$$\omega_{\frac{1}{2}}^2 = \frac{-i\omega_R^2 \omega_p^2 k_{xR} x_0 [1 - r(\omega_R)][1 - q(\omega_R)]}{2\gamma_p^3(\omega_{pl}^2 - \omega_R^2)[q(\omega_R) - r(\omega_R)]}\,, \tag{18}$$

with $r(\omega_R) = b(\omega_R)/a(\omega_R)$, $q(\omega_R) = d(\omega_R)/c(\omega_R)$ and where k_{xR} is either of the two solutions for k_x evaluated at $\omega = \omega_R$. There are four solutions for $\omega_{\frac{1}{2}}$ and solving (18) for k_{xR} determines the appropriate sign of k_{xR} for each solution. For the choice $b(\omega) = c(\omega) = 0$, the above reproduces the planar geometry calculations of RR99 and these shall not be discussed further here.

Choosing instead the Bessel function forms of A95

$$B^r(\omega, \rho) = A(\omega) H_\nu^{(1,2)}(k_r x_0 \rho)\,, \qquad B^l(\omega, \rho) = C(\omega) J_\nu(k_r x_0 \rho)\,, \tag{19}$$

with $A(\omega)$ and $C(\omega)$ arbitrary functions of ω, $\nu = mW^{\frac{1}{2}}$ and $k_r = \omega W^{\frac{1}{2}}/c$ and where $H_\nu^{(1,2)}$ is either Hankel function, we obtain (with $\rho_- = 1$)

$$\omega_{\frac{1}{2}}^2 = -\epsilon \frac{i\pi\omega_p^2 m^2 \beta^2}{2\gamma_p^3} H_\nu^{(1,2)\prime}(\nu\beta) J_\nu'(\nu\beta)\,, \tag{20}$$

where $\beta = x_0\Omega/c$ with $\epsilon = +1$ for $H_\nu^{(1)}$ and $\epsilon = -1$ for $H_\nu^{(2)}$ and with primes denoting differentiation with respect to the argument. All quantities on the right-hand side are evaluated at $\omega = \omega_R$. Although (20) was derived for magnetic fields relevant to a global cylindrical geometry, it can also be obtained in planar geometry with the choice of $a(\omega)$, $b(\omega)$, $c(\omega)$ and $d(\omega)$ made such that the magnetic field at the beam boundaries agrees with (19) and the actual beam geometry is irrelevant to this order (see also Section 5). This result is more general than that given by APS83 and A95 and applies for small $|\nu|$ as well as large $|\nu|$ (although not for $|\nu| \sim 0$). The solutions can be categorised as either short or long wavelength (as defined in RR99) and in the remainder of this paper we consider only the former, which can be compared directly with the results of APS83 and A95.

Short-wavelength Waves

Short-wavelength waves as defined by RR99 satisfy $\omega_R \geq \omega_{pl}$, in which case ν evaluated at $\omega = \omega_R$ is real (without loss of generality we take $\nu > 0$). Defining the real positive quantity

$$N_\nu = \left\{ J'_\nu(\nu\beta)^2 + Y'_\nu(\nu\beta)^2 \right\}^{\frac{1}{2}} \ , \tag{21}$$

one can write the real and imaginary parts of $\omega_{\frac{1}{2}}$ explicitly:

$$\mathrm{Re}[\omega_{\frac{1}{2}}] = \pm\, \frac{\pi^{\frac{1}{2}}\omega_p m\beta}{2\gamma_p^{\frac{3}{2}}} |J'_\nu|^{\frac{1}{2}} \left[\left(\frac{N_\nu + J'_\nu}{2} \right)^{\frac{1}{2}} + \left(\frac{N_\nu - J'_\nu}{2} \right)^{\frac{1}{2}} \right], \tag{22}$$

$$\mathrm{Im}[\omega_{\frac{1}{2}}] = \mp\, \epsilon \frac{\pi^{\frac{1}{2}}\omega_p m\beta}{2\gamma_p^{\frac{3}{2}}} |J'_\nu|^{\frac{1}{2}} \left[\left(\frac{N_\nu + J'_\nu}{2} \right)^{\frac{1}{2}} - \left(\frac{N_\nu - J'_\nu}{2} \right)^{\frac{1}{2}} \right], \tag{23}$$

where all square roots are positive real and the prime denotes differentiation of the Bessel functions with respect to the argument $\nu\beta$, which we have omitted for brevity. It can be shown that for $0 < \beta < 1$ the function $J'_\nu(\nu\beta) \geq 0$ for all positive real ν and hence the final factors in (22) and (23) (in brackets) are positive.

If $|\nu|$ is large the lowest order terms in an expansion in Airy functions (e.g. Abramowitz and Stegun 1965) give an approximation which lends itself more readily to numerical evaluation than do (22) and (23). Using

$$H_\nu^{(1,2)'}(\nu\beta) \sim -\, \frac{2^{\frac{1}{2}}}{\beta\gamma_p^{\frac{1}{2}}\nu^{\frac{2}{3}}\zeta^{\frac{1}{4}}} \left[Ai'(\nu^{\frac{2}{3}}\zeta) - \epsilon i Bi'(\nu^{\frac{2}{3}}\zeta) \right], \tag{24}$$

$$J'_\nu(\nu\beta) \sim -\, \frac{2^{\frac{1}{2}} Ai'(\nu^{\frac{2}{3}}\zeta)}{\beta\gamma_p^{\frac{1}{2}}\nu^{\frac{2}{3}}\zeta^{\frac{1}{4}}} \,, \tag{25}$$

with

$$\zeta = (\tfrac{3}{2})^{\frac{2}{3}} \left[\tfrac{1}{2} \ln\left(\frac{\gamma_p + 1}{\gamma_p - 1} \right) - \frac{1}{\gamma_p} \right]^{\frac{2}{3}} , \tag{26}$$

and defining the positive real quantity

$$R = \{Ai'(\nu^{\frac{2}{3}}\zeta)^2 + Bi'(\nu^{\frac{2}{3}}\zeta)^2\}^{\frac{1}{2}} \tag{27}$$

gives

$$\mathrm{Re}[\omega_{\frac{1}{2}}] = \pm \frac{\pi^{\frac{1}{2}}\omega_p m}{2^{\frac{1}{2}}\zeta^{\frac{1}{4}}\gamma_p^2\nu^{\frac{2}{3}}} |Ai'|^{\frac{1}{2}} \left[\left(\frac{R - Ai'}{2}\right)^{\frac{1}{2}} + \left(\frac{R + Ai'}{2}\right)^{\frac{1}{2}} \right], \tag{28}$$

$$\mathrm{Im}[\omega_{\frac{1}{2}}] = \mp \epsilon \frac{\pi^{\frac{1}{2}}\omega_p m}{2^{\frac{1}{2}}\zeta^{\frac{1}{4}}\gamma_p^2\nu^{\frac{2}{3}}} |Ai'|^{\frac{1}{2}} \left[\left(\frac{R - Ai'}{2}\right)^{\frac{1}{2}} - \left(\frac{R + Ai'}{2}\right)^{\frac{1}{2}} \right], \tag{29}$$

where the prime denotes differentiation of the Airy functions with respect to argument $\nu^{\frac{2}{3}}\zeta$ which we have omitted for brevity. In equations (24) to (29) principal roots are taken.

One may approximate further when $\nu^{\frac{2}{3}}\zeta$ is also small (corresponding to γ_p large so that $\zeta \sim 2^{-\frac{2}{3}}\gamma_p^{-2}$), by taking only the lowest orders for the Airy function

$$Ai'(\nu^{\frac{2}{3}}\zeta) \approx -\frac{Bi'(\nu^{\frac{2}{3}}\zeta)}{3^{\frac{1}{2}}} \approx -\frac{1}{3^{\frac{1}{3}}\Gamma(\frac{1}{3})}, \tag{30}$$

in which case

$$\omega_{\frac{1}{2}} = \pm \frac{2^{\frac{1}{6}}}{3^{\frac{1}{3}}} \left(\frac{3^{\frac{1}{2}} + 1}{2} - \epsilon i \frac{3^{\frac{1}{2}} - 1}{2} \right) \frac{\pi^{\frac{1}{2}}\omega_p m^{\frac{1}{3}}}{\gamma_p^{\frac{3}{2}}\Gamma\left(\frac{1}{3}\right) W^{\frac{1}{3}}}, \tag{31}$$

where again principal roots are meant. This reproduces results of A95 and APS83 in an explicit form, specifically equation (104) of A95 for the case $W \sim 1$, corresponding to a beam bounded on both sides by rarefied plasma. As mentioned above, this result can also be derived using the fields (15) and (16) relevant to planar geometry with the appropriate choice of coefficients $a(\omega)$ to $d(\omega)$ and implies that the results to this order are independent of the actual beam geometry.

5. Discussion

From Maxwell's equations one obtains an equation for the wave energy averaged over a wave period. For waves of the form (3) and (5), propagating in a medium of infinite extent characterised by the dielectric tensor of Section 2 with real k_z, the time averaged wave energy equation is

$$2\omega_i \overline{\mathcal{W}} + \nabla \cdot \overline{\boldsymbol{\mathcal{P}}} = 0, \tag{32}$$

where ω_i is the imaginary part of ω, and $\overline{\mathcal{W}} = \overline{\mathcal{W}}_{EM} + \overline{\mathcal{W}}_p$ is the total wave energy. Further

$$\overline{\mathcal{W}}_{EM} = \frac{\varepsilon_0}{4} \left[|E_y(\omega,\rho)|^2 + c^2 \left(1 + \frac{c^2 k_y^2}{|\omega|^2}\right) |B_z(\omega,\rho)|^2 \right] \exp(2\omega_i t) \tag{33}$$

is the time averaged electromagnetic energy,

$$\overline{\mathcal{W}}_p = \frac{\varepsilon_0}{4}\frac{\omega_p^2}{\gamma_p^3}\frac{(|\omega|^2 - \omega_R^2)}{|\omega - \omega_R|^4}|E_y(\omega,\rho)|^2 \exp(2\omega_i t) \tag{34}$$

is the time averaged energy in forced particle motions and

$$\overline{\boldsymbol{\mathcal{P}}} = \frac{1}{2\mu_0}\left(\mathrm{Re}[E_y^*(\omega,\rho)B_z(\omega,\rho)]\hat{\boldsymbol{x}} + \frac{c^2 k_y \omega_r}{|\omega|^2}|B_z(\omega,\rho)|^2\hat{\boldsymbol{y}}\right)\exp(2\omega_i t) \tag{35}$$

is the electromagnetic or Poynting flux with ω_r the real part of ω. As $\boldsymbol{K}(\omega,\boldsymbol{k})$ does not depend on k_x or k_z the forced particle energy flux $\overline{\boldsymbol{F}}_p$ is directed along the $\hat{\boldsymbol{y}}$ axis and, given that k_y is real, does not appear in (32) because $\nabla\cdot\overline{\boldsymbol{F}}_p = 0$. The above forms for $\overline{\mathcal{W}}_{EM}$, $\overline{\mathcal{W}}_p$ and $\overline{\boldsymbol{\mathcal{P}}}$ apply for a planar geometry, however the cylindrical geometry forms are obtained by making replacements as before (see the discussion below equation 5).

(5a) Conditions for Instability

For waves satisfying $|\omega|^2 > \omega_R^2$, then $\overline{\mathcal{W}}_p > 0$ and the waves can grow only if $\nabla\cdot\overline{\boldsymbol{\mathcal{P}}} < 0$, corresponding to an influx of electromagnetic energy into a given volume V. Such growing waves do not represent instabilities. Similarly waves with $|\omega|^2 > \omega_R^2$ are damped only if $\nabla\cdot\overline{\boldsymbol{\mathcal{P}}} > 0$, corresponding to an outflow of electromagnetic energy from V. For waves satisfying $|\omega|^2 < \omega_R^2$, however, $\overline{\mathcal{W}}_p < 0$ and the total wave energy may be negative. In that case the waves can grow with $\nabla\cdot\overline{\boldsymbol{\mathcal{P}}} > 0$, corresponding to an outflux of electromagnetic energy from V and indicating a *reactive* instability. Similarly reactive damping is possible with $\nabla\cdot\overline{\boldsymbol{\mathcal{P}}} < 0$ implying an influx of electromagnetic energy into V. The condition $|\omega|^2 < \omega_R^2$ is satisfied provided $\omega_i^2 < \omega_R^2$ and

$$-(\omega_R^2 - \omega_i^2)^{\frac{1}{2}} < \omega_r < (\omega_R^2 - \omega_i^2)^{\frac{1}{2}} < |\omega_R|\,. \tag{36}$$

Thus a necessary but not sufficient condition for a reactive instability is that the real part of the frequency shift $\delta\omega_r = \omega_r - \omega_R$ be negative [as was pointed out by Buschauer and Benford (1979) and RR99].

In the bounded beam system, regarding the beam as infinitesimally thin and integrating (32) over the beam thickness a, we obtain

$$2\omega_i\overline{\mathcal{W}}_s - \Delta\overline{\boldsymbol{\mathcal{P}}}_x = 0\,, \tag{37}$$

where $\Delta\overline{\mathcal{P}}_x = \overline{\mathcal{P}}_x^l - \overline{\mathcal{P}}_x^r$ is the discontinuity of the normal component of the Poynting flux across the thin surface layer and

$$\overline{\mathcal{W}}_s = a\overline{\mathcal{W}} \approx a\overline{\mathcal{W}}_p \approx \frac{\varepsilon_0}{2}\frac{\omega_p^2 a}{\gamma_p^3}\frac{\omega_R\delta\omega_r}{|\delta\omega|^4}|E_y(\omega,\rho)|^2\exp(2\omega_i t) \tag{38}$$

is the total wave energy in the beam (or surface layer between the bounding plasmas). This is dominated by the energy in forced particle motions and is of $O(a^{-\frac{1}{2}})$ for $\delta\omega \sim a^{\frac{1}{2}}$. In this approximation it is clear that for waves with $\delta\omega_r < 0$ the total wave energy in the beam is always negative and a reactive instability ($\omega_i > 0$) corresponds to a net electromagnetic flux out of the beam, that is $\Delta\overline{\mathcal{P}}_x < 0$. Similarly reactive damping ($\omega_i < 0$) corresponds to a net electromagnetic energy flux into the beam, $\Delta\overline{\mathcal{P}}_x > 0$.

(5b) Near Fields

We now consider the Poynting flux in the near field region (specifically at the beam interface) of short-wavelength waves, assuming wavefields of the form (19) close to the beam. In cylindrical coordinates the Poynting flux in the bounding plasma to the right of the beam is, to lowest order,

$$\overline{\boldsymbol{\mathcal{P}}} \approx \frac{1}{\mu_0}\left[\epsilon\frac{1}{m\pi W}\hat{\boldsymbol{r}} + \tfrac{1}{2}|H_\nu^{(1,2)}(\nu\beta)|^2\hat{\boldsymbol{\phi}}\right]\frac{c\gamma_p}{(\gamma_p^2-1)^{\frac{1}{2}}}|A(\omega_R)|^2\exp(2\omega_i t)\,, \tag{39}$$

with quantities on the right-hand side evaluated at $\omega = \omega_R$. The wave frequency shift is given by (22) and (23) and choosing the upper signs gives Re $\omega_{\frac{1}{2}} > 0$ and Im $\omega_{\frac{1}{2}} \lessgtr 0$ for $\epsilon = \pm 1$ (corresponding to $H_\nu^{(1)}$ and $H_\nu^{(2)}$ respectively). As discussed above, the real part of the frequency shift being positive implies that the waves are not unstable. The temporally growing solution ($\epsilon = -1$) corresponds to an influx of wave energy from infinity, while the temporally decaying solution ($\epsilon = +1$) corresponds to radiation of wave energy away from the beam to infinity. Choosing the lower signs gives Re $\omega_{\frac{1}{2}} < 0$ and Im $\omega_{\frac{1}{2}} \gtrless 0$ for $\epsilon = \pm 1$. These solutions correspond to reactive instability with outward Poynting flux, and reactive decay with inward Poynting flux respectively, and are thus similar to the long-wavelength modes B^+ and B^- of RR99.

For near fields of the assumed form, the Poynting flux to the left of the beam is away from the beam for the temporally growing waves and towards the beam for the temporally damped waves. This is clear for a cylindrical geometry: in that case this bounding plasma is enclosed by the beam (as suggested by Fig. 1) and the beam is its only source or sink of wave energy.

(5c) Far Fields

The results obtained in this paper show that the wave frequency and growth or damping rate for thin beam solutions are determined entirely by the wave fields at the beam interface (the near fields), independent of the beam geometry. The form of the far field and its interpretation, however, depends on the particular global geometry/symmetry assumed; however, in applications such as to pulsars, a simple global geometry is difficult to justify and so the corresponding far fields may not be relevant to such applications. We consider the far fields below, in planar and cylindrical geometry, for completeness.

In a global cylindrical geometry, the choice (19) for the wavefields implies a far field ($\rho \to \infty$) of the form

$$B_z(\omega,\rho) = A(\omega)\left(\frac{2}{\pi k_r x_0 \rho}\right)^{\frac{1}{2}}\exp\{\epsilon i(k_r x_0\rho - (2\nu+1)\pi/4)\}\,. \tag{40}$$

The Poynting flux on the right-hand side of the beam to lowest order is

$$\overline{\boldsymbol{\mathcal{P}}} \approx \frac{1}{2\mu_0}\left[\epsilon\frac{1}{W^{\frac{1}{2}}}\hat{\boldsymbol{r}} + \frac{\gamma_p}{(\gamma_p^2-1)^{\frac{1}{2}}}\hat{\boldsymbol{\phi}}\right] c|B_z(\omega_R,\rho)|^2\exp(2\omega_i t)\,, \tag{41}$$

where quantities on the right-hand side are evaluated at $\omega = \omega_R$ and with

$$|B_z(\omega,\rho)|^2 = \left(\frac{2}{\pi|k_r|x_0\rho}\right)|A(\omega)|^2\exp\{-2\epsilon(k_{ri}x_0\rho - \nu_i\pi/2)\}\,, \tag{42}$$

where $\nu_i = \mathrm{Im}[\nu]$, and in the short-wavelength regime $k_{ri} = \mathrm{Im}[k_r] = \omega_i W^{\frac{1}{2}}/c$ (k_r was defined after equation 19). In this case, the Poynting flux of the far field has the same directional sense as that of the near field. The wave amplitude drops off exponentially with increasing distance ρ from the beam for the reactive growth/damping cases which have $\epsilon\omega_i > 0$ (implying that the beam is a source/sink of radiation), and increases with ρ for the non-reactive growth/damping cases which have $\epsilon\omega_i < 0$ (implying that there is essentially a source/sink of radiation in the far field).

In a global planar geometry the near field has the form (19) for the choices

$$a(\omega) = \tfrac{1}{2}\left[H_\nu^{(1,2)}(k_r x_0) - i\frac{k_r}{k_x}H_\nu^{(1,2)\prime}(k_r x_0)\right]A(\omega), \tag{43}$$

$$b(\omega) = \tfrac{1}{2}\left[H_\nu^{(1,2)}(k_r x_0) + i\frac{k_r}{k_x}H_\nu^{(1,2)\prime}(k_r x_0)\right]A(\omega)\,, \tag{44}$$

in (15), and the near field Poynting flux is then the same as (39). The far field ($\rho \to \infty$) has the form

$$B_z(\omega,\rho) = a(\omega)\exp\{ik_x(\rho-1)x_0\}\,, \tag{45}$$

where we assume without loss of generality that for the imaginary part of k_x, we have $k_{xi} < 0$. For short-wavelength waves ($\omega_R > \omega_{pr}$) the Poynting flux to lowest orders is

$$\overline{\boldsymbol{\mathcal{P}}} = -\frac{\omega_i\overline{\mathcal{W}}_{EM}}{|k_{xR}|}\hat{\boldsymbol{x}} + \frac{1}{2\mu_0}\,\frac{c^2k_y}{\omega_R}\,|B_z(\omega,\rho)|^2\exp(2\omega_i t)\hat{\boldsymbol{y}}\,, \tag{46}$$

with quantities on the right-hand side evaluated at $\omega = \omega_R$ and where

$$|B_z(\omega,\rho)|^2 = |a(\omega)|^2\exp\{-2k_{xi}(\rho-1)x_0\}\,. \tag{47}$$

In this case the Poynting flux in the far field is directed towards the beam for *both* the reactive and non-reactive temporally growing modes and away from the beam for both damping modes, with exponential growth of the wave amplitude with increasing ρ in all cases. The exponential growth and the direction of the Poynting flux imply that there is a source/sink of radiation in the far field in the temporally growing/damping cases, irrespective of whether or not the growth/damping at the beam is reactive. In the reactive cases, this also implies that the Poynting flux changes direction somewhere between the near field and far field regions.

6. Conclusions

In this paper we have considered the stability of a thin-beam of monoenergetic electrons and positrons. Considering the beam as an infinitesimally thin interface between the bounding plasmas, we have derived a general result for the growth/damping rates and frequency shift which is equally applicable to planar and cylindrical geometry. The result indicates that thin-beam growth/damping rates depend only on the values of the electromagnetic fields at the interface and not explicitly on the geometry of the beam; that is, the local beam geometry is irrelevant. Our general result was obtained in a straightforward manner and we explicitly reproduced previous results of planar and cylindrical geometry in a geometry independent way. In the 'cylindrical' case we have provided a more general result than appears elsewhere. We interpret this result by considering the stability criteria for the beam and calculating the Poynting flux in the near and far field regions. The determination of the Poynting flux in the far field is geometry dependent and leads to different interpretations for global planar and cylindrical geometries. The far field considerations may not be relevant to applications such as pulsar radio emission, as simple global geometries are not plausible.

References

Abramowitz, M., and Stegun, I. A. (1965). 'Handbook of Mathematical Functions' (Dover: New York).
Asséo, E. (1995). *Mon. Not. R. Astron. Soc.* **276**, 74–102.
Asséo, E., Pellat, R., and Sol, H. (1983). *Astrophys. J.* **266**, 201–14.
Buschauer, R., and Benford, G. (1978). *Mon. Not. R. Astron. Soc.* **185**, 493–506.
Buschauer, R., and Benford, G. (1979). *Phys. Fluids* **22**, 1297–1305.
Goldreich, P., and Keeley, D. A. (1971). *Astrophys. J.* **170**, 463–77.
Rowe, G. W., and Rowe, E. T. (1999*a*). *J. Plasma Phys.* **62**, 425–39.
Rowe, G. W., and Rowe, E. T. (1999*b*). *J. Plasma Phys.* **62**, 441–8.

Manuscript received 10 August, accepted 24 November 1999